Surface phase transitions in nematic liquid crystals with planar anchoring

R. Seidin and R. M. Hornreich
Physics of Complex Systems, Weizmann Institute of Science, 76100 Rehovot, Israel

D. W. Allender
Department of Physics and Liquid Crystal Institute, Kent State University, Kent, Ohio 44242

(Received 17 October 1994; revised manuscript received 10 January 1996)

We calculate the thermodynamic phase diagram of a semi-infinite nematic liquid crystal system above its bulk ordering temperature for the case of planar boundary conditions. The latter are assumed to favor a uniaxially ordered surface state, characterized by a negative orientational order parameter, at sufficiently high temperatures. All symmetry-allowed terms either linearly or quadratically proportional to the tensor order parameter characterizing the transition to a biaxially ordered surface state are included in the analysis. The Euler-Lagrange equations obtained by minimizing the Landau–de Gennes free energy expression are solved exactly by numerical methods. We find that both first- and second-order transitions are possible; they occur in different sections of the thermodynamic phase boundary separated by a line of tricritical points. In the second-order region, we evaluate the effect of fluctuations on this quasi-two-dimensional system by introducing the Berezinskii-Kosterlitz-Thouless mechanism, and calculating its effect on the phase boundary and nature of the transition. Possible ways of observing this phase transition experimentally are considered and some potentially useful techniques noted. [S1063-651X(97)09103-4]

PACS number(s): 64.70.Md, 61.30.Cz

I. INTRODUCTION

The effect of a bounding surface upon nematic liquid crystal (NLC) ordering has been of interest for both fundamental and technological reasons. In the former area, NLC's have been utilized as relatively simple model systems in which different types of interactions between a bounding surface and anisotropic molecules can be studied. Technologically, fixing the orientation of liquid crystal molecules at cell surfaces is a key element in the design of display devices, and must therefore be properly understood and controlled.

As a consequence of the above interests, a great deal of experimental and theoretical work has been carried out in order to understand the influence of nematic-surface interactions on local ordering at an interface. It has become apparent that the symmetry breaking which occurs at a surface leads to a variety of interesting phenomena, including surface-induced ordering and phase transitions between surface-oriented states.

Theoretically, the nematic-solid boundary has been investigated primarily for the simplest types of surface interactions; namely, those preferentially orienting the molecules either normal or parallel to the surface. Three distinct surface orientations are, in principle, possible.

(a) *Homeotropic* alignment, wherein the preferred molecular orientation is normal to the surface. In this case, the surface interaction is necessarily invariant under all rotations about an axis normal to the surface and the latter is a principal axis of the alignment.

(b) *Homogeneous* alignment, wherein the preferred orientation is along an axis lying in the surface. Here both the normal and the preferred in-plane axis are principal axes.

(c) *Planar* alignment, wherein the molecules lie preferentially in the surface plane, but lack a preferred orientation. In this case, the invariance of the surface interaction is the same as in (a), but the axis of the molecules is normal to the principal axis of the alignment. This configuration is described by a negative orientational order parameter.

The homogeneous case is common experimentally, but little has been done theoretically regarding the formation of surface layers. The homeotropic case has been studied theoretically by several researchers [1–3] who found a temperature-surface coupling phase diagram which resembled that of a positive anisotropy bulk NLC phase diagram in the temperature-applied field plane [4]. Later, Schick [5] pointed out that this phase diagram can be described using the language of wetting [6,7]. Experimentally, Miyano [8] was the first to observe surface-induced order in NLC's at temperatures above the nematic-isotropic (NI) transition temperature, T_{NI}. In another experimental study, Chen *et al.* [9] studied the wetting behavior of the NLC homologous series of alkyl cyanobiphenyls, nCB, $n=5$, 6, 7, 8, and 9 (n served as a practical way of tuning the strength of the NLC-surface interaction), using an evanescent wave ellipsometry technique. Their results showed partial orientational wetting of the surface for the case of 5CB [10] and complete wetting for 6CB to 9CB. The complete wetting behavior became more apparent as n was increased.

Theoretically, a traceless second-rank tensor is an appropriate macroscopic description of the order parameter for the case of a NLC. Among possible choices, an experimentally convenient one is obtained by taking the position-dependent dielectric tensor $\epsilon_{ij}^{D}(\mathbf{x})$ and subtracting one-third of its trace from each of its main diagonal elements. The desired order parameter $\epsilon_{ij}(\mathbf{x})$ is thus given by [1]

$$\epsilon_{ij}=\epsilon_{ij}^{D}-\frac{1}{3}\mathrm{Tr}(\boldsymbol{\epsilon}^{D})\,\delta_{ij}\,. \tag{1}$$

This tensor is symmetric, and can be diagonalized in its prin-

cipal axis basis at any point **x**. If any two of the resulting eigenvalues are equal, the system is said to be *uniaxial*. Otherwise, it is *biaxial*. Clearly, if the system is everywhere uniaxial above a specific temperature, then a symmetry-breaking phase transition occurs when biaxiality appears below this temperature.

In terms of ϵ_{ij}, the standard Landau–de Gennes expression for the bulk free energy density, which is assumed to be valid in the vicinity of the NI phase transition is [11,12]

$$g_b[\boldsymbol{\epsilon}]=\tfrac{1}{2}[a\epsilon_{ij}^2+c_1\epsilon_{ij,k}^2+c_2\epsilon_{ij,i}\epsilon_{kj,k}]-\beta\epsilon_{ij}\epsilon_{jk}\epsilon_{ki}+\gamma(\epsilon_{ij}^2)^2. \tag{2}$$

Here $\epsilon_{ij,k}\equiv\partial\epsilon_{ij}/\partial x_k$ and all repeated indices are summed over. Only the coefficient a is regarded as (linearly) temperature dependent; the other coefficients ($\beta,\gamma,\ c_1$, and c_2) are taken to be constant in the temperature region of interest.

The above expression for g_b can be simplified by introducing the following scaled parameters [13]:

$$\mu_{ij}=(\beta/\sqrt{6}\gamma)\epsilon_{ij},\quad \tfrac{1}{4}t=(3\gamma/\beta^2)a,\quad f=(36\gamma^3/\beta^4)g,$$

$$\tfrac{1}{4}\xi^2=(3\gamma/\beta^2)c_1,\quad \rho=c_2/c_1. \tag{3}$$

Here, in particular, t is a reduced temperature variable with $t=1$ corresponding to $T=T_{\rm NI}$, and ξ sets the length scale over which the order parameter magnitude changes in the z direction. It will characterize the thickness of the ordered surface layer. Because the bend elastic constant of nematics is typically twice the value of the twist constant, the physically reasonable range of ρ is of order one. Realistic choices of the other parameters are discussed in Sec. II D.

In terms of these parameters, the scaled bulk free energy density becomes

$$f_b[\boldsymbol{\mu}]=\tfrac{1}{4}[t\mu_{ij}^2+\xi^2(\mu_{ij,k}^2+\rho\mu_{ij,i}\mu_{kj,k})]$$
$$-\sqrt{6}\mu_{ij}\mu_{jk}\mu_{ki}+(\mu_{ij}^2)^2. \tag{4}$$

To obtain the total scaled free energy density, we must supplement f_b by a similarly scaled *surface* contribution f_s. We shall be concerned, in this work, with a semi-infinite system bounded, at $z=0$, by a flat surface upon which *planar boundary conditions* apply. To second order in the reduced order parameter μ_{ij}, the scaled surface free energy density is given by [14,15]

$$f_s[\boldsymbol{\mu}]=[\nu\mu_{33}+\tfrac{1}{2}(-\nu_1\mu_{\alpha\beta}\mu_{\alpha\beta}+\nu_2\mu_{ij}\mu_{ji}+\nu_3\mu_{3i}\mu_{i3})]$$
$$\times\xi\delta(z-z_0), \tag{5}$$

where $\alpha,\beta=1,2$, and z_0 is an arbitrarily small offset which insures that the surface interaction is in the half-space $z>0$. Only one term linear in the order parameter is allowed for planar boundary conditions; it is given by the ν term in f_s. The other three terms are the symmetry-allowed quadratic contributions. If the analysis is restricted to phases in which the surface normal is one of the principal axes of μ_{ij}, the ν_3 term in $f_s[\boldsymbol{\mu}]$ is not independent of those proportional to ν_1 and ν_2, and may therefore be suppressed. This will be done henceforth. In addition, it will be assumed that all order parameter configurations of interest are uniform in the x-y plane. The relations between the rescaled surface parameters (ν,ν_1,ν_2) and the real physical quantities are given in Sec. III.

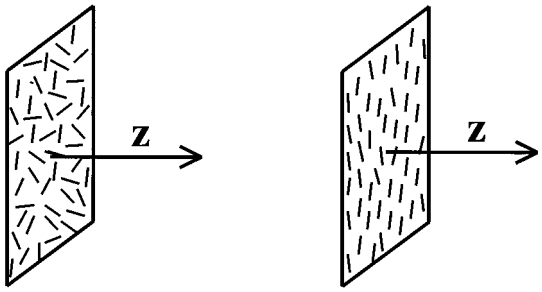

FIG. 1. Schematic views of the semi-infinite space occupied by the liquid nematic liquid crystal system. The left side illustrates the molecular distribution on the bounding surface for the case of in-plane isotropic ordering; the right side shows the equivalent distribution when the in-plane symmetry is broken.

The total scaled free energy per unit area in the x-y plane is now

$$F[\boldsymbol{\mu}]=F_b[\boldsymbol{\mu}]+F_s[\boldsymbol{\mu}]=\int_0^\infty dz\ f_b+\int_0^\infty dz\ f_s. \tag{6}$$

Both integrals converge for all $t>1$. The physical system is shown schematically in Fig. 1.

Since the scaled order parameter μ_{ij} is a symmetric traceless tensor, it can, at any point **x**, be diagonalized in a local principal axis system in terms of two scalar functions $\mu(z)$ and $\eta(z)$. That is, we can write

$$\boldsymbol{\mu}(\mathbf{x})=\boldsymbol{\mu}(z)$$
$$=\frac{1}{\sqrt{6}}\begin{bmatrix}-\mu(z)+\eta(z) & 0 & 0\\ 0 & -\mu(z)-\eta(z) & 0\\ 0 & 0 & 2\mu(z)\end{bmatrix}. \tag{7}$$

The functions $\mu(z)$ and $\eta(z)$ are determined by minimizing F for any particular system. Note that when $\eta(z)=0$ or $\pm3\mu(z)$, the phase is uniaxial; otherwise, it is biaxial.

In this work we obtain the surface phase diagram for the case of planar anchoring, characterized by a negative surface orientational order state which arises due to the random planar molecular alignment. Experimentally, the negative surface orientational order state was observed both using an evanescent wave elipsometry technique [16] and using deuterium NMR [17].

The first workers to theoretically discuss the possibility of having surface-induced biaxial order in NLC's with planar boundary conditions were Sluckin and Poniewierski (SP) [14,18]. They used a Landau–de Gennes formalism in which the coefficient c_1 in the bulk free energy [see Eq. (2)] was set equal to zero [or equivalently, $\rho\to\infty$ in Eq. (4)]. Further, only the linear surface coupling term [proportional to ν—see Eq. (5)] was included in $f_s[\boldsymbol{\mu}]$. A phase transition to a biaxially ordered surface state above $T_{\rm NI}$ was obtained by requiring that ν be positive. An interesting feature of the phase diagram was the existence of a line of continuous

phase transitions from a high-temperature uniaxial surface state to a biaxial one. SP noted that the order in the surface biaxial layer has the same symmetry as in the two-dimensional XY model. This phase transition, which describes symmetry breaking within the bounding plane, is therefore in principle described by the Berezinskii-Kosterlitz-Thouless (BKT) [19–21] mechanism. It was argued by SP that their neglect of the c_1 elasticity term in the Landau–de Gennes bulk free energy did not change the topology of the phase diagram. On the other hand, however, the addition of quadratic surface coupling terms could lead to changes in its topology [18].

The case of finite ρ was stuided by L'vov, Hornreich, and Allender [22], and, later, Kothekar, Allender, and Hornreich [23]. They obtained, for physically interesting values of ρ ($\simeq 1$), the correct Landau theory surface phase diagram in the (t-ν) phase plane, and also calculated the BKT transition boundary due to fluctuation effects. Kothekar, Allender, and Hornreich showed numerically that a transition to a biaxial phase does not occur for sufficiently large ν when $\rho \lesssim 0$. An analytic proof that this crossover point is exactly at $\rho = 0$ is given by us in Appendix A.

A first attempt to go beyond the linear term approximation for the surface coupling was made by Hornreich, Kats, and Lebedev [24] who, however, considered *only* the quadratic surface term proportional to $\nu_1 > 0$ (to favor in-plane molecular orientation) in the scaled surface free energy [i.e., they set $\nu = \nu_2 = 0$ in Eq. (5)]. In our work, we broadened these earlier studies by considering a more realistic model. Specifically, we included in the scaled surface free energy terms both linear and quadratic in μ_{ij} [see Eq. (5)]. Experimentally, both types of terms are always present, and their relative magnitudes cannot be fixed independently. It is therefore important to determine whether the uniaxial-biaxial surface phase transition reported in the series of papers discussed above occurs under conditions which, experimentally, are more realistic. We used Eqs. (4) and (5) for the scaled bulk and surface free energy densities, respectively. Our analysis was restricted to configurations in which the surface normal was a principal axis of the tensor order parameter. Therefore, without loss of generality, we could set $\nu_3 = 0$. Note that, to our knowledge, this is the first study in which *both* linear and quadratic surface terms are included in the analysis, and the additional symmetry-allowed ν_2 contribution to the scaled surface free energy is explicitly considered.

Our study was carried out in two steps. In the first, we ignored the ν_2 term in the scaled surface free energy density, considering only the contributions proportional to ν and ν_1. The complete mean-field phase diagram in the (t-ν-ν_1) thermodynamic space was then obtained for $t > 1$ by *exactly* solving the coupled nonlinear Euler-Lagrange differential equations for the order parameter with appropriate boundary conditions. This was done numerically by employing a software code (COLNEW) [25,26] specifically developed to solve such problems (multipoint boundary value problems for a coupled system of ordinary differential equations). The long wavelength in-plane fluctuations characteristic of BKT phase transitions were then considered, and their effects upon the mean-field phase diagram calculated.

In the second step, the fully isotropic surface contribution proportional to ν_2 was also considered. It was shown that this term does *not* change the topology of the surface phase diagram, but simply shifts the transition boundary by an amount essentially proportional to the magnitude and sign of ν_2.

The outline of our paper is as follows: In Sec. II A, we present the general Landau theory framework for our calculation, including the details of the surface interaction potential being considered. Some technical points regarding the numerical procedure employed to solve the coupled nonlinear differential equations describing the equilibrium states are noted. Next, in Sec. II B, a restricted surface interaction potential is considered, and the associated thermodynamic phase diagram calculated. In Sec. II C, we return to the general expression for the surface potential, and show that the results of Sec. II B are essentially unchanged. Then, in Sec. II D, the role played by thermodynamic fluctuations near the phase transition is analyzed and shown to result in a two-dimensional transition of the BKT type. A phase boundary appropriate to this type of transition is calculated and compared with that obtained from the mean-field Landau theory. Finally, in Sec. III, we discuss our results, compare them with those reported in earlier work, and consider possible ways of verifying them experimentally. Technical details are given in two appendices.

II. THEORY

A. Landau theory in the general case

As discussed in Sec. I, we are interested in a NLC system which fills the half-space $z > 0$ and interacts via a surface potential with the $z = 0$ boundary (see Fig. 1). Assuming that the surface interactions are short range in character, the total free energy of the system is well modeled by integrating over a sum of bulk and surface free energy densities f_b and f_s, which are given in a suitably scaled Landau–de Gennes formalism in Eqs. (4) and (5). When no bulk ordering is present (i.e., $t > 1$) and the relevant order parameter configurations are uniform in the x-y plane, the total scaled free energy is given by Eq. (6).

Again noting that the term in f_s proportional to ν_3 [see Eq. (5)] does not contribute when z is a principal axis of the order parameter $\mu_{ij}(z)$, we substitute Eq. (7) into Eqs. (4)–(6) and obtain

$$F_b/\xi = \int_0^\infty d\zeta \left[\tfrac{1}{4} t \mu^2 - \mu^3 + \mu^4 + \tfrac{1}{4}\left(1 + \tfrac{2}{3}\rho\right)(\mu')^2 + \mu \eta^2 + \tfrac{2}{3}\mu^2 \eta^2 + \tfrac{1}{12} t \eta^2 + \tfrac{1}{9} \eta^4 + \tfrac{1}{12} (\eta')^2 \right], \tag{8}$$

$$F_s/\xi = \left[\frac{2}{\sqrt{6}} \nu \mu_0 + \left(-\tfrac{1}{6}\nu_1 + \tfrac{1}{2}\nu_2\right)\mu_0^2 + \tfrac{1}{6}\left(-\nu_1 + \nu_2\right)\eta_0^2 \right]. \tag{9}$$

Here $\mu_0 = \mu(z=0)$, $\eta_0 = \eta(z=0)$, $\zeta = z/\xi$ is a reduced coordinate in the z direction, and a prime denotes derivation with respect to ζ.

It will be convenient to use new surface coupling constants which are linear combinations of ν_1 and ν_2. We shall call them $\tilde{\nu}_1$ and $\tilde{\nu}_2$ and define them in terms of the original parameters by

$$\tilde{\nu}_1 = \nu_1 - \nu_2, \tag{10a}$$

$$\tilde{\nu}_2 = \tfrac{2}{3}\nu_2. \tag{10b}$$

In terms of these new parameters, the η_0^2 term in Eq. (9) is dependent only upon $\tilde{\nu}_1$ and *not* upon $\tilde{\nu}_2$, while the μ_0^2 term in this equation has the same functional form, with ν_1 and ν_2 now replaced by $\tilde{\nu}_1$ and $\tilde{\nu}_2$, respectively. Further, from Eq. (10), when $\nu_2 = 0$, $\nu_1 = \tilde{\nu}_1$.

The equilibrium order parameter components $\mu(\zeta)$ and $\eta(\zeta)$ are determined by minimizing $F = F_b + F_s$ with respect to μ and η. This yields two coupled, nonlinear, differential Euler-Lagrange equations

$$(1+\tfrac{2}{3}\rho)\mu'' = t\mu - 6\mu^2 + 8\mu^3 + 2\eta^2 + \tfrac{8}{3}\mu\eta^2, \tag{11a}$$

$$\eta'' = t\eta + \tfrac{8}{3}\eta^3 + 12\mu\eta + 8\mu^2\eta. \tag{11b}$$

While $\eta = 0$ is a trivial solution of these equations (with appropriate boundary conditions—see below), it is not always the thermodynamically stable state, i.e., the configuration minimizing the free energy.

Since we are interested in the regime $t > 1$ where no bulk ordering occurs, the order parameter describing the system asymptotically approaches that of the disordered or isotropic state far from the $\zeta = 0$ boundary. The boundary conditions at $\zeta = \infty$ are therefore

$$\mu(\zeta = \infty) = \mu'(\zeta = \infty) = 0, \tag{12a}$$

$$\eta(\zeta = \infty) = \eta'(\zeta = \infty) = 0. \tag{12b}$$

The $\zeta = 0$ boundary conditions are obtained by integrating the variational equations in an infinitesimal region about this point. This procedure yields [22,24,27]

$$\mu'(\zeta = 0) = \frac{2}{(1+\frac{2}{3}\rho)}\left[\frac{2}{\sqrt{6}}\nu + (-\tfrac{1}{3}\tilde{\nu}_1 + \tilde{\nu}_2)\mu_0\right], \tag{13a}$$

$$\eta'(\zeta = 0) = -2\tilde{\nu}_1\eta_0. \tag{13b}$$

When both linear and quadratic surface terms are present, Eqs. (11), together with the accompanying boundary conditions, Eqs. (12) and (13), cannot be solved analytically. In order to solve this coupled pair of nonlinear differential equations, we therefore employed COLENEW [25,26]. However, in order to efficiently utilize the COLENEW procedure when solving coupled differential equations with boundary conditions at infinity, one must take care to avoid solutions which grow exponentially as ζ increases. An effective way of doing this is to replace the boundary conditions in Eqs. (12) by [25,26]

$$\mu'(\overline{\zeta}) = \frac{\sqrt{t}}{\sqrt{1+\frac{2}{3}\rho}}\mu(\overline{\zeta}), \tag{14a}$$

$$\eta'(\overline{\zeta}) = \sqrt{t}\,\eta(\overline{\zeta}), \tag{14b}$$

where $\overline{\zeta}$ is a large but otherwise arbitrary value of ζ.

Exact numerical solutions of the Euler-Lagrange equations, together with their accompanying boundary conditions, were found in two stages. In the first, the isotropic term ν_2 was arbitrarily set equal to zero. This corresponds to a direct combination of the two cases considered previously, i.e., those in which the bounding potential was described by either a ν [14,18,22,23] or a ν_1 [24] surface term. The results from this part of our study can thus be directly compared with those reported previously. Subsequently, the effect of including a nonzero ν_2 term on the phase diagram was considered.

B. Case $\nu_2 = 0$

We now consider the special case in which only two (ν, $\nu_1 = \tilde{\nu}_1$) of the three allowed surface coupling parameters are nonzero. The third (ν_2) will be taken equal to zero in this part of the analysis. This does not affect the expression for the bulk scaled free energy, which remains as in Eq. (8). From Eqs. (9) and (10), however, the scaled surface free energy reduces to

$$F_s/A\xi = \frac{2}{\sqrt{6}}\nu\mu_0 - \tfrac{1}{6}\tilde{\nu}_1\mu_0^2 - \tfrac{1}{6}\tilde{\nu}_1\eta_0^2. \tag{15}$$

The surface couplings ν and $\tilde{\nu}_1$ are taken to be positive. As noted, this restricted model includes, as special cases, those studied previously by Hornreich, Kats, and Lebedev [24], where only the quadratic surface coupling $\tilde{\nu}_1$ was considered (i.e., $\nu = \tilde{\nu}_2 = 0$, so that $\tilde{\nu}_1 = \nu_1$) and that extensively analyzed by Sluckin and Poniewierski [14,18], L'vov, Hornreich, and Allender [22], and Kothekar, Allender, and Hornreich [23], where only the linear surface coupling was included (i.e., $\nu_1 = \nu_2 = 0$). As we shall see, adding the quadratic $\tilde{\nu}_1$ term to the linear surface coupling one in F_s tends to favor biaxial ordering in the thermodynamic phase space, thereby expanding the region in this space in which a biaxially ordered surface state is energetically preferred. This is due to the final term in Eq. (9), which couples $\tilde{\nu}_1$ to the biaxial order at the surface. It provides the mechanism whereby biaxial ordering, under appropriate conditions, lowers the system's free energy.

As noted, the Euler-Lagrange equations (11) cannot be solved analytically. We therefore solved this pair of coupled non-linear differential equations for $\mu(\zeta)$ and $\eta(\zeta)$ numerically using COLENEW [25,26]. This code is invoked via a simple calling routine, which includes as subroutines the differential equations to be solved and the boundary conditions at the endpoints. In our case, these are given by Eqs. (11) and (13) (with $\tilde{\nu}_2 = 0$), and Eq. (14). In the latter, we set $\zeta = 20$. Employing the COLENEW procedure carefully, we succeeded in obtaining accurate results for the thermodynamic boundaries separating the different states in the phase diagram, and also in distinguishing between first- and second-order phase transitions. Our procedure was to first consider a point in the (t-ν-$\tilde{\nu}_1$) phase space known to be well within the biaxial region. The exact numerical solution

was then calculated at this point without the need for an initial guess for the magnitude of the order parameter components. Then the temperature was increased by a small amount (the surface coupling parameters remaining fixed) and the solution at this point found by using the previous solution at the neighboring point as an initial guess. This procedure was repeated until, eventually, the phase boundary separating the biaxial surface phase region from that of the uniaxial surface phase was approached.

When the phase transition was second order for the particular surface couplings being considered, a smooth continuous change from a solution with $\eta \neq 0$ to one with $\eta = 0$ was obtained. However, when it was first order, a point was reached at which the COLENEW algorithm no longer converged. In this case, the transition point was determined by also using COLENEW to compute the uniaxial ($\eta = 0$) solution in the temperature region just below that at which biaxial convergence ended. By comparing the total free energies per unit surface area of the two solutions, the thermodynamic phase boundary was fixed as the temperature at which these two values were equal.

After a transition point was found, the values of the surface couplings were changed by a small amount, and an initial temperature deep in the biaxial region was selected. The procedure described above was then repeated until the new transition point was reached. Finally, the locus of the transition points gave the uniaxial-biaxial phase boundary.

Note that if the starting point is taken in the uniaxial region (i.e., where the $\eta = 0$ solution is stable) and the above procedure of using the results for one temperature as the initial guess for the next one is followed, then, upon decreasing the temperature, one continues to obtain the ''trivial'' uniaxial solution in the biaxial region even when it is no longer the energetically preferred solution. The temperature at which this uniaxial state is replaced by the biaxial one as the thermodynamic ground state can then be determined only by comparing the free energies of the two solutions.

Our results are summarized graphically in Figs. 2(a)–2(d). All were obtained using COLENEW and setting $\rho = 1$. [Physically, ρ is of $O(1)$ and the phase diagram is not very sensitive to the actual value of ρ in this range; $\rho = 1$ was chosen as a representative value.] Figure 2(a) is a three-dimensional rendition of the phase boundary, in the (t-ν-$\tilde{\nu}_1$) thermodynamic space, between the high-temperature uniaxial phase and the biaxial surface state. Note that (1) on part of the phase boundary (dark grey in the figure) the uniaxial-biaxial transition is first-order, elsewhere it is second-order (light gray); (2) the phase boundary intercepts the $\nu = 0$ plane when $\tilde{\nu}_1 \gtrsim 1$; and (3) as expected (see Appendix A), when $\nu \to \infty$ with $\tilde{\nu}_1$ fixed, the boundary becomes asymptotically parallel to the bulk critical plane $t = 1$.

Cuts of the phase boundary for fixed values of $\tilde{\nu}_1$ are given in Figs. 2(b) and 2(c). The boundary's asymptotic behavior as $\nu \to \infty$ is seen clearly in Fig. 2(b) and the line of tricritical points separating the first- and second-order regions is shown explicitly in Fig. 2(c). We see that, at small ν, the transition is first order; as ν increases, it becomes second order via a tricritical point. The latter ''slides'' down the surface as $\tilde{\nu}_1$ is increased, finally reaching the $\nu = 0$ plane [see the inset of Fig. 2(a)] when $\tilde{\nu}_1 \simeq 1$. For $\tilde{\nu}_1 \gtrsim 1$, the uniaxial-biaxial phase boundary is second-order for all ν values.

As noted, for small $\tilde{\nu}_1$ values, the surface phase boundary meets the $t = 1$ bulk critical plane at a nonzero (though small) value of ν. The ν value at this intersection point decreases with increasing $\tilde{\nu}_1$, reaching zero at $\tilde{\nu}_1 \approx 0.3$. For $\tilde{\nu}_1 \gtrsim 0.3$, the transition boundary no longer intersects the $t = 1$ plane. This can be seen particularly clearly in Fig. 2(d), where we show (t - $\tilde{\nu}_1$) plane cuts of the phase boundary for fixed values of ν.

C. Effect of the isotropic surface term

As noted in Sec. II A, the expression for the scaled surface free energy used in Sec. II B was restricted because one of the symmetry-allowed coupling parameters ν_2 was taken to be zero. Here we remove this restriction and consider the general case, i.e., Eq. (9) with all three parameters (ν, ν_1, and ν_2 or, equivalently, ν, $\tilde{\nu}_1$, and $\tilde{\nu}_2$) nonzero.

Inspecting Eq. (9), we see that the general expression for the surface scaled free energy differs from Eq. (15) only in the coefficient of μ_0^2, where $(-\frac{1}{6}\tilde{\nu}_1)$ is replaced by $(-\frac{1}{6}\tilde{\nu}_1 + \frac{1}{2}\tilde{\nu}_2)$ when the isotropic term is included. Thus no qualitative (topological) changes in the thermodynamic phase diagram found in Sec. II B and summarized in Fig. 2 are expected. Numerical solutions of the Euler-Lagrange equations for the general case confirmed this. As an example, we show, in Fig. 3, the results obtained using COLENEW when the third surface coupling parameter $\tilde{\nu}_2$ is included in the calculation. Here $\tilde{\nu}_1$ was fixed (at a value of 0.5). As expected, the phase boundaries previously obtained for the case $\tilde{\nu}_2 = 0$ [see Figs. 2(a) and 2(b)] shift in accordance with the sign and magnitude of $\tilde{\nu}_2$, but the topological structure of the surface phase diagram is unchanged.

D. Effect of fluctuations

The thermodynamic phase diagrams given in Figs. 2 and 3 were obtained by using the Landau–de Gennes formalism, and solving the differential equations minimizing the total free energy. This procedure, of course, neglected thermodynamic fluctuations and is therefore a mean-field solution of the model. Since, however, we have seen that the transition to a biaxial phase can be second order, it follows that fluctuations can have a significant effect on the thermodynamic phase boundaries. Indeed, such fluctuations are expected to be particularly relevant as the system is essentially two dimensional in character near the onset of the transition to a biaxially ordered phase, where the relevant in-plane correlation length will be significantly greater than the layer thickness. Consequently, we expect, for given surface coupling coefficients, that the biaxial phase boundary actually occurs at a lower temperature than that given by the mean-field field solution, and no longer has a mean-field character. We therefore evaluate, in this section, the effect of these fluctuations upon the phase diagram.

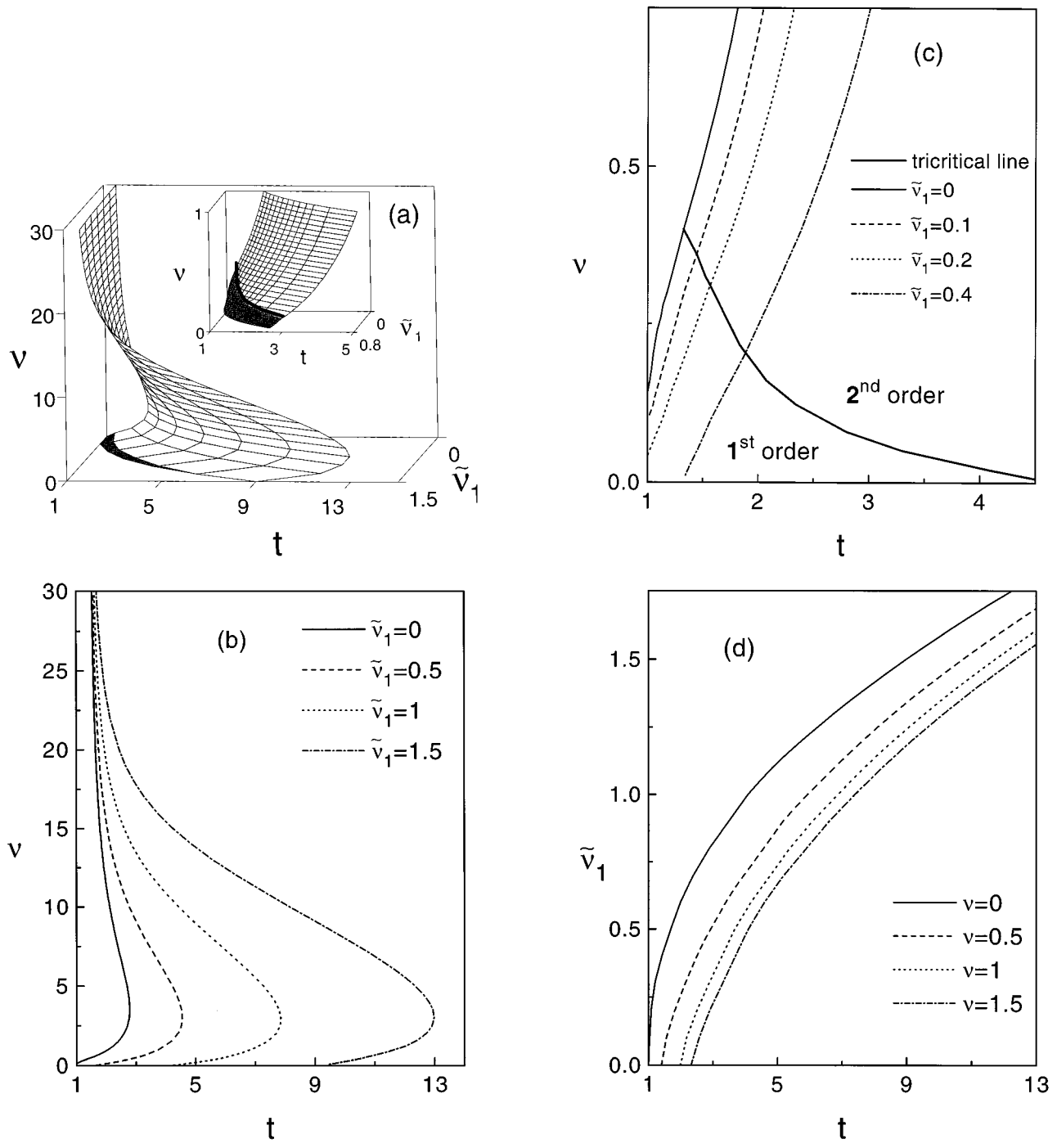

FIG. 2. Surface phase diagram in the $(t\text{-}\nu\text{-}\tilde{\nu}_1)$ thermodynamic space from exact Landau theory calculations. (a) Full three-dimensional diagram. (b) and (c) $(t\text{-}\nu)$ plane cuts. (d) $(t\text{-}\tilde{\nu}_1)$ plane cuts.

As we are interested in surface phase transitions occurring within a layer whose thickness remains finite, it follows that these are basically two dimensional in character. Then, according to the theory of BKT [19–21], the relevant fluctuations which must be taken into account near the phase boundary are long-wavelength in-plane phase variations of the symmetry-breaking order parameter. The latter (η) becomes non-zero in the biaxial phase.

In the BKT theory, the long-wavelength fluctuations are characterized by an effective stiffness K_b, and the part of the (unscaled) free energy associated with these fluctuations is given by [20,29]

$$G_{\mathrm{BKT}}=\tfrac{1}{2}K_b\int dx\,dy(\nabla\theta)^2, \tag{16}$$

where $(\nabla\theta)^2=(\partial_x\theta)^2+(\partial_y\theta)^2$ and θ is the local angle in the x-y plane between a principal axis of the order parameter and a fixed in-plane direction. We now put the relevant part of the fluctuation-sensitive free energy of the NLC system in the form of Eq. (16), thereby obtaining an expression for K_b in terms of the parameters introduced by us in Eq. (2). Consider, therefore, the biaxial part η of the order parameter as given in Eq. (7). The in-plane fluctuations can be de-

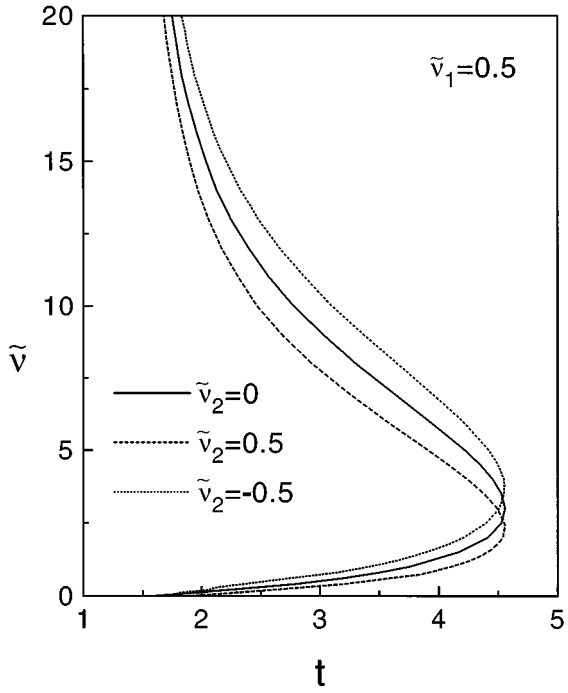

FIG. 3. Surface phase diagram obtained from exact Landau theory calculations when the additional isotropic term in the surface free energy, proportional to $\tilde{\nu}_2$, is considered.

scribed by local variations of the angle $\theta(x,y)$ defined above and the in-plane fluctuating part of the order parameter, $\boldsymbol{\mu}_{\rm fluct}$, can be written as

$$\boldsymbol{\mu}_{\rm fluct}=\begin{bmatrix}\cos\theta & -\sin\theta\\ \sin\theta & \cos\theta\end{bmatrix}\frac{1}{\sqrt{6}}\begin{bmatrix}\eta(\zeta) & 0\\ 0 & -\eta(\zeta)\end{bmatrix}\begin{bmatrix}\cos\theta & \sin\theta\\ -\sin\theta & \cos\theta\end{bmatrix}$$
$$=\frac{1}{\sqrt{6}}\eta(\zeta)\begin{bmatrix}\cos 2\theta & \sin 2\theta\\ \sin 2\theta & -\cos 2\theta\end{bmatrix}. \tag{17}$$

The free energy associated with phase fluctuations is found by substituting Eq. (17) into the gradient (i.e., elastic) terms in the (unscaled) bulk free energy Eq. (2). Using Eqs. (3) and (4), the latter may be written as

$$G_{\rm fluct}=\left[\frac{\beta^4}{36\gamma^3}\right]\frac{\xi^2}{4}\int d^3x(\mu_{ij,k}^2+\rho\mu_{ij,j}\mu_{ik,k}). \tag{18}$$

Substituting Eq. (17) into Eq. (18) and using Eq. (3), for the free energy associated with the long-wavelength in-plane fluctuations we obtain

$$G_{\rm fluct}=\frac{1}{2}\left[\frac{2}{9}\frac{\beta^2}{\gamma^2}c_1(1+\tfrac{1}{2}\rho)\xi\int_0^\infty d\zeta\ \eta^2(\zeta)\right]\int dx\ dy(\nabla\theta)^2. \tag{19}$$

Comparing Eqs. (16) and (19), we find that the effective stiffness K_b for our model is given by

$$K_b=\frac{2}{9}\frac{\beta^2}{\gamma^2}c_1(1+\tfrac{1}{2}\rho)\xi\int_0^\infty d\zeta\ \eta^2(\zeta), \tag{20}$$

where ξ, β, γ, c_1, and $\rho=c_2/c_1$ are material-dependent constants whose values can be deduced from experimental results [28]. Given K_b, the phase transition temperature T_s of the BKT model is obtained from the relation

$$\lim_{T\to T_s^-} K_b=\frac{8}{\pi}k_BT_s. \tag{21}$$

The factor 8 is due to the invariance of the system's order parameter with respect to π rather than 2π rotations, as is the case for a conventional magnet [29]. Also, we have neglected the renormalization of K_b due to the presence of bound disclination pairs in the biaxial state [20,29]. Given the other approximations made and the estimates to be used for the various parameters, this is reasonable.

The BKT phase transition boundary was calculated as follows: For the parameters in K_b, we used values taken from the literature [3,28,30] and given in Ref. [22], i.e., $\beta=2.4\times10^7$ ergs/cm^3, $\gamma=2.2\times10^7$ ergs/cm^3, and $c_1=13.5\times10^{-7}$ erg/cm. These gave $\xi=7.9\times10^{-7}$ cm. We assumed that T_s was approximately equal to $T_{\rm NI}=350$ K [i.e., $(T_s-T_{\rm NI})/T_{\rm NI}\ll1$] and, as elsewhere, that $\rho=1$. For fixed coupling parameters and temperature, the order parameter $[\mu(\zeta),\eta(\zeta)]$ in the biaxial phase was found and the effective elastic constant K_b at this point was calculated. Then, by scanning in the t direction for fixed values of the coupling parameters, the scaled temperature at which Eq. (21) is satisfied was found.

The results of our calculations are summarized in Fig. 4. In Figs. 4(a) and 4(b), two-dimensional (t-ν) plane cuts of the phase diagram are shown, for $\tilde{\nu}_1=0.5$ and 1.5, respectively, and $\tilde{\nu}_2=0$. For comparison purposes, both BKT and Landau theory results for the phase transition line are given. Figures 4(c) and 4(d) are also (t-ν) plane cuts, with $\tilde{\nu}_1=0.5$ and 1, respectively. In both, we show BKT phase boundaries for $\tilde{\nu}_2=0$ and 0.5 and, for comparison, the Landau theory transition line for $\tilde{\nu}_2=0$. Finally, in Figs. 4(e) and 4(f), (t-$\tilde{\nu}_1$) plane cuts showing both BKT and Landau boundaries for $\nu=0.5$ and 1.5, respectively, and $\tilde{\nu}_2=0$ are given. From the figures, the shift to lower temperatures of the transition boundary between the uniaxially and biaxially ordered surface phases from the Landau (mean-field) position for all values of the surface interaction coupling parameters is clearly evident.

III. DISCUSSION

In this study, we have considered the most general symmetry-allowed interaction possible between a NLC system and a planar bounding surface, subject to two conditions. These are (a) the coupling constants are either linearly or quadratically proportional to the magnitudes of components of the tensor order parameter at the interface, and (b) the normal to the surface is a principal axis of the order parameter. We thus disregard, in particular, nonlocal couplings, e.g., those dependent upon the values of derivatives of the order parameter at the interface [31], and the additional coupling term appearing in tilt configurations, where a principal axis of the order parameter makes an acute angle with the surface normal. As regards the former, we note that such terms are expected to be negligible in our geometry [32]. The

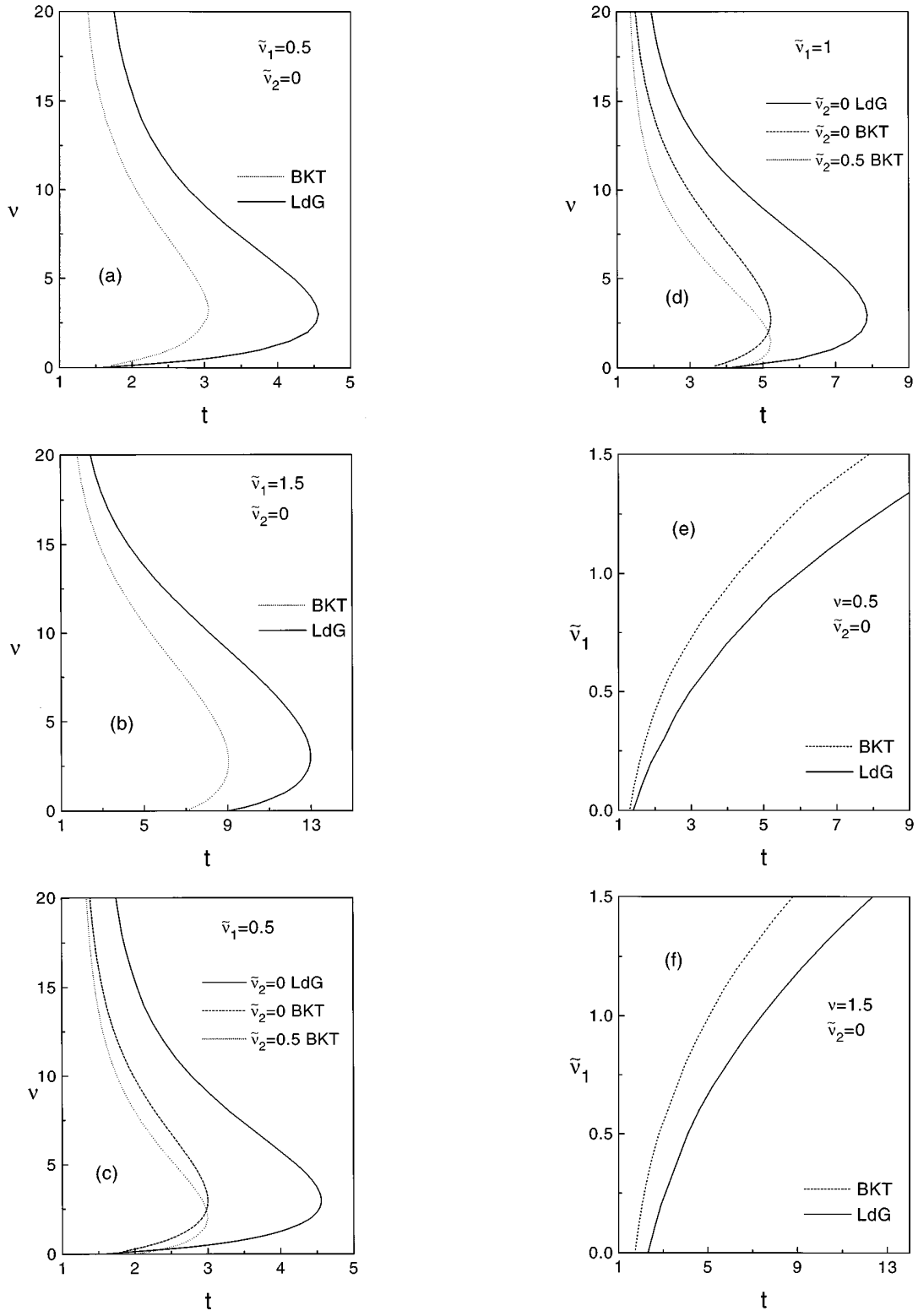

FIG. 4. Modified surface phase diagram obtained from the Berezinskii-Kosterlitz-Thouless (BKT) theory of two-dimensional phase transition. Parts (a) and (b) are (t-ν) plane cuts for $\tilde{\nu}_1=0.5$ and 1.5, respectively, and $\tilde{\nu}_2=0$. Parts (c) and (d) are also (t-ν) plane cuts; here the effect of the isotropic term in the surface free energy, proportional to $\tilde{\nu}_2$, on the BKT boundary is considered. We present the results for $\tilde{\nu}_2=0.5$ and $\tilde{\nu}_1=0.5$ and 1, respectively. Parts (e) and (f) are (t-$\tilde{\nu}_1$) plane cuts for $\nu=0.5$ and 1.5, respectively, and $\tilde{\nu}_2=0$. In all the figures, both BKT and Landau theory results are shown.

latter is also not of central importance as our main objective is to examine the conditions under which BKT-type phase transitions can occur in a NLC surface layer.

For the interaction potentials that we considered, the surface contribution to the free energy is expressed phenomenologically in terms of three parameters [14,15]. All previous work studying planar boundary conditions [14,18,22–24] dealt, at different levels of approximation, with only a single

parameter, most often that linearly proportional to an order parameter component [14,18,22,23]. Only in one study [24] was a quadratic coupling parameter considered.

The mean-field results of Kothekar, Allender, and Hornreich [23] for the surface phase diagram were obtained by minimizing the free energy exactly using COLENEW. The BKT phase boundary was then calculated by the same method discussed in Sec. II D. Kothekar, Allender, and Hornreich [23] were able to resolve the open questions remaining from earlier limited and approximate studies [14,18,22] of the same free energy functional.

Hornreich, Kats, and Lebedev [24] used only a single quadratic surface interaction potential (proportional to $\nu_1=\tilde{\nu}_1$) to model the surface free energy. In addition, only three limiting configurations for the allowed phases were considered: an isotropic or disordered state, a strictly uniaxial one, and a completely biaxial structure. It was shown, under these conditions, that a continuous isotropic-to-biaxial phase transition should occur when ν_1 is greater than some minimum value. Even for the model considered, their surface phase diagram was approximate, as the mean-field Euler-Lagrange variational equations were not solved exactly, and the BKT phase boundary was found by calculating the fluctuation-induced shift from the mean-field transition line.

The principal results obtained by us here are presented in Figs. 2–4. In all calculations, the elastic constant ratio was $\rho=1$. We found that the phase diagram was not sensitive to this parameter as long as its value was physically reasonable (i.e., in the range $0\lesssim\rho\lesssim 2$). Of course, for $\tilde{\nu}_1=\tilde{\nu}_2=0$, our results reduce to those of Ref. [23]. However, for $\nu=\tilde{\nu}_2=0$, our results differ from those reported earlier by Hornreich, Kats, and Lebedev [24]. This is due (as they themselves noted) to the constrained nature of the order parameters considered by them. Thus, where they found regions in which ordered surface states with different symmetries (uniaxial and fully biaxial) were respectively preferred, we find only a *single* ordered state, characterized by biaxial order. Of course, this order parameter approaches that of a fully biaxial state in the region in which Hornreich, Kats, and Lebedev found the latter state and, conversely, approaches uniaxiality where those authors reported a stable uniaxial state. Further, we find that the ordered surface state exits only when $\tilde{\nu}_1$ exceeds a minimum value, and that there is an interval of $\tilde{\nu}_1$ values (beginning at the minimum value noted and terminating at a tricritical value) for which the transition between the isotropic or fully disordered state and the biaxially ordered surface state is of first-order. The authors of Ref. [24], whose analytic calculations considered only the *stability limit* of their uniaxial state ansatz, were not sensitive to either of these possibilities.

In Figs. 2(b)–2(d), we present two-dimensional cuts of the three-dimensional thermodynamic space (t-ν-$\tilde{\nu}_1$) shown in Fig. 2(a). As expected, we find that a phase transition from the $\tilde{\nu}_1\neq 0$ high-temperature uniaxial phase (which is bounded by the fully isotropic phase when $\tilde{\nu}_1=0$) to the biaxially ordered surface phase occurs at a temperature $t>1$ for almost all values of the coupling parameters $[\nu,\tilde{\nu}_1]$. Only where *both* parameters are sufficiently small does no transition occur. For somewhat higher $[\nu,\tilde{\nu}_1]$ values, there is a region in which the transition is first order; this region is bounded by a line of tricritical points. For higher values of $[\nu,\tilde{\nu}_1]$, the transition from the high temperature to the biaxial phase is continuous. Ultimately (see Appendix A), the continuous transition boundary to the biaxial phase becomes asymptotically parallel to the $t=1$ plane as $\nu\rightarrow\infty$ for all $\tilde{\nu}_1$. Note particularly that the second-order transition between the high-temperature uniaxial phase and the biaxially ordered surface state occurs for a wide range of $[\nu,\tilde{\nu}_1]$ values; this, of course, is very desirable as it increases the possibility of observing this phase transition experimentally.

The effect of including $\tilde{\nu}_2$ in the theoretical model is to shift the $\tilde{\nu}_2=0$ thermodynamic phase boundary shown in Fig. 2(a), but not to change it in any significant way. As illustrated in Fig. 3, the phase boundary shifts in accordance with the sign and magnitude of $\tilde{\nu}_2$, but its form as a function of ν and $\tilde{\nu}_1$ is essentially preserved. Thus the influence of this particular coupling parameter on the phase diagram is less than that of the other two considered in our analysis.

Since all Landau theory calculations are necessarily mean field in character, our calculations were extended to include fluctuation effects. This was done by recognizing that, in the critical region, the system is essentially two dimensional in character and that, consequently, the BKT theory is applicable. We therefore modified the Landau model calculation by taking the relevant long-wavelength variations of the order parameter into account, as discussed in Sec. II D. The results are summarized in Fig. 4, where different two-dimensional cross sections of the thermodynamic phase diagram are given. At first glance, there are no qualitative differences between the BKT and Landau theory results for the phase boundary; the most obvious effect of the fluctuations is to lower the temperature at which the transition occurs for a given surface coupling parameter values. However, there is a second, more significant, difference as the BKT model is particular to two-dimensional systems. In this case, the biaxial phase does *not* exhibit true long-range order with a nonzero order parameter (as it does in the mean-field Landau theory) but is instead characterized by algebraic decay of correlation functions. This is a property which one would wish to confirm experimentally.

In order to compare our theoretical results with possible experiments, it is necessary to recast the scaled parameters defining the theoretical phase diagram into physical quantities. Typical values for the bulk parameters of NLC's are given in Sec. II D; from these and experimental studies it follows that the reduced unit of temperature $t=1$ is of the order of 0.5 to 1 K [13]. The scaled surface interaction coupling parameters ν, ν_1, and ν_2 can be related to physical values by defining the latter via the expression

$$g_s[\boldsymbol{\epsilon}]=(\sigma\epsilon_{33}-\tfrac{1}{2}\sigma_1\epsilon_{\alpha\beta}\epsilon_{\alpha\beta}+\tfrac{1}{2}\sigma_2\epsilon_{ij}\epsilon_{ij})\,\delta(z-z_0). \quad (22)$$

Comparing Eqs. (5) and (22) and using Eq. (3), we obtain relations between the scaled and physical surface free energy parameters. These are

$$\sigma=\frac{\beta^3\xi}{6\sqrt{6}\,\gamma^2}\,\nu, \qquad \sigma_{1,2}=\frac{\beta^2\xi}{6\gamma}\,\nu_{1,2} \quad (23)$$

Using the β, γ, and ξ values cited in Sec. II D, we find that $\sigma=\nu\times 1.5$ ergs/cm^2, and $\sigma_{1,2}=\nu_{1,2}\times 3.4$ ergs/cm^2. These relations therefore define the range of surface couplings required in order to observe the theoretically predicted BKT surface phase transition. Reported experimental measurements [22,24,33,34] indicate that surfaces characterized by interaction potentials appropriate to observing the predicted phase transition can be prepared.

One possible experimental technique for observing the BKT surface transition is evanescent-wave ellipsometry, as developed by Chen *et al.* [10]. Here one measures the phase difference Δ between p- and s-polarized light incident upon a liquid crystal-substrate interface and totally reflected at the critical angle. This phase difference is proportional to the integrated birefringence in the surface plane of the ordered surface layer and can therefore be used, in principle, to detect the phase transition since the biaxial phase is birefringent while the uniaxial one is not. The (mean-field) Landau–de Gennes theory gives

$$\Delta\sim\int_0^\infty d\zeta\ \eta(\zeta)\sim(t_{\rm ub}-t)^{1/2}, \tag{24}$$

where the final expression is valid for t slightly less than $t_{\rm ub}$, the reduced uniaxial-biaxial transition temperature calculated from the theory. Thus the critical behavior of Δ appears only through its $(t_{\rm ub}-t)$ dependence. This, of course, is expected as this technique probes a static property of the system and is consequently sensitive only to static critical properties. Since the deviation from this simple square root dependence for Δ when the transition is of the BKT type is subtle, it would be difficult to verify such a character for the phase transition by this approach.

To see this, consider the effect of fluctuations on the behavior of our system near the BKT phase transition temperature T_s. It is well known that, in this region, all thermodynamic quantities scale as powers of the correlation length ξ_+ (defined as the length over which order persists for $T>T_s$), which has an essential singularity at T_s of the form [20,21]

$$\xi_+=\xi\ \exp\left[\frac{C}{(T-T_s)^{1/2}}\right],\quad T>T_s. \tag{25}$$

Here C is a positive constant. For $T<T_s$, $\xi_+=\infty$. As a consequence of the essential (rather than more usual power law) character of the singularity, modifications in the static critical behavior characteristic of BKT transitions are difficult to detect experimentally.

A better approach would be to study the dynamics of the critical behavior by light scattering techniques, as discussed by Hornreich, Kats, and Lebedev [24]. We review the theory applicable to this technique in Appendix B.

In summary, we have calculated the thermodynamic phase diagram of a semi-infinite nematic liquid crystal system above its bulk ordering temperature for the case of planar boundary conditions. It was assumed that the latter favor a uniaxially ordered surface state characterized by a negative orientational order parameter, at sufficiently high temperatures. All symmetry-allowed terms either linearly or quadratically proportional to the tensor order parameter characterizing a transition to a biaxial state were included in the analysis. The Euler-Lagrange equations obtained by minimizing the Landau–de Gennes expression for the free energy were solved exactly by numerical means. For the region in which the transition was found to be of second order, we considered the effect of fluctuations on this quasi-two-dimensional system by introducing the Berezinskii-Kosterlitz-Thouless mechanism and evaluating its effect on the phase boundary. The possibilities for observing this phase transition experimentally were considered and some potentially useful techniques noted.

ACKNOWLEDGMENTS

This work was supported in part by the National Science Foundation under Science and Technology Center ALCOM DMR89-20147 and the Basic Research Foundation, administered by the Israeli Academy of Arts and Sciences, Jerusalem, Israel. We acknowledge helpful discussions with E. C. Gartland regarding the use of COLENEW. One of the authors (R.M.H.) was a visitor at the Liquid Crystal Institute, Kent State University, during part of the period in which this work was done.

APPENDIX A: ASYMPTOTIC BEHAVIOR OF THE BIAXIAL PHASE TRANSITION BOUNDARY AS $\nu\to\infty$

Motivated by the numerical results [23] showing, for $\rho\lesssim 0$ and $\tilde{\nu}_1=\tilde{\nu}_2=0$, that a biaxial surface state does not exist for $t>1$ when ν exceeds a maximum value $\nu_{\rm max}(\rho)$, we reanalyzed the Euler-Lagrange equations (11) and associated boundary conditions, Eqs. (12) and (13), in an attempt to determine $\nu_{\rm max}(\rho)$ analytically. To do this, we set $t=1$ and $\tilde{\nu}_1=\tilde{\nu}_2=0$, and linearize Eqs. (11) in η and its derivatives (since the uniaxial-biaxial surface phase transition is expected to be second-order), and obtain

$$(1+2\rho/3)\mu''=\mu-6\mu^2+8\mu^3, \tag{A1a}$$

$$\eta''=\eta(1+12\mu+8\mu^2). \tag{A1b}$$

The boundary conditions at $\zeta=\infty$ are as given in Eqs. (12); those at $\zeta=0$ are given by Eqs. (13) with $\tilde{\nu}_1=\tilde{\nu}_2=0$. Setting $(1+2\rho/3)=s^2$ (note that $\rho>-\frac{3}{2}$ always [13]), the solution of Eqs. (A1a), (12a), and (13a) is

$$\mu(\zeta)=\tfrac{1}{2}[1-\phi^{-1}\exp(\zeta/s)]^{-1}, \tag{A2}$$

with $\phi^{-1}=(1-1/2\mu_0)$ and $\mu_0\equiv\mu(\zeta=0)=\frac{1}{4}[1-(1+32\nu/\sqrt{6}s)^{1/2}]$. In the physical domain $0\leq\zeta\leq\infty$, $\mu(\zeta)<0$, and $0\leq\phi\leq 1$.

Defining $\tau=[1-\phi\ \exp(-\zeta/s)]$ and using Eq. (A2), Eq. (A1b) becomes

$$\tau^2(1-\tau)^2\eta_{\tau\tau}-\tau^2(1-\tau)\eta_\tau-s^2(2-10\tau+9\tau^2)\eta=0, \tag{A3a}$$

with the associated boundary conditions

$$\eta_\tau(\tau=1-\phi)=\eta(\tau=1)=0. \tag{A3b}$$

The physical domain is now $1-\phi\leq\tau\leq 1$, $\eta_\tau\equiv d\eta/d\tau$, etc.

Equation (A3a) is a second-order linear differential equation for η with regular singular points at $\tau=0$ and 1. The boundary condition $\eta(\tau=1)=0$ ensures that $\eta\sim(1-\tau)^s A_0(\tau)$, where $A_0(\tau)$ goes to a (nonzero) constant value as $\tau\to 1$. However, in the neighborhood of $\tau=0$, we have

$$\eta\sim A_1(\tau)\tau^{r_1}+A_2(\tau)\tau^{r_2}, \tag{A4}$$

where $r_{1,2}=(1\pm\sqrt{1+8s^2})/2$, and $A_{1,2}(\tau)$ are functions of τ and the parameter $(1-s)$. Since $r_1>0$ and $r_2<0$, the behavior of η at small τ is determined by whether $A_2(\tau)$ is greater than, equal to, or less than zero as $\tau\to 0^+$. In general, the values of $A_{1,2}$ are evaluated by continuing these functions into the region near the $\tau=1$ singular point. The value of $\nu_{\max}$ is then obtained by determining the value of ϕ such that $\eta_\tau(\tau=1-\phi)=0$.

A particularly interesting special case is $\rho=0$ or $s=1$. Here $A_2(\tau)$ is identically zero and the *exact solution* of Eq. (A3a), valid for $0\leqslant\tau\leqslant 1$, is $\eta=\tau^2(1-\tau)$. Since $\eta_\tau(\tau=0)=0$, the boundary condition $\eta_\tau(\tau=1-\phi)=0$ yields $\phi=1$. This in turn gives $\mu_0\to-\infty$ and $\nu\to\nu_{\max}\to\infty$. We therefore conclude that $\nu_{\max}=\infty$ at $\rho=0$.

Further analysis shows that $A_2(\tau)$ is positive for $-\frac{3}{2}<\rho<0$, and negative for $\rho>0$. Consequently, $\nu_{\max}$ is finite for $-\frac{3}{2}<\rho<0$. Its approximate value in this range is $\nu_{\max}(\rho)\simeq\sqrt{6}s(1-Q)/8Q^2$, with $Q\simeq 0.223(1-s)^{1/3}$.

APPENDIX B: LIGHT SCATTERING AT SURFACE PHASE TRANSITIONS

As in Sec. II D, we parametrize the long-wavelength fluctuations of the symmetry-breaking two-dimensional order parameter η by the angular variable $\theta(x,y,t)=\theta(\mathbf{r},t)$. The time dependence is now written explicitly and $\mathbf{r}$ is an x-y plane position vector. For $T>T_s$, the BKT mechanism results in a finite density of free disclinations which inhibit ordering in the surface layer. It is therefore necessary to take these disclinations into account. This has been done for smectic-A–C transitions in freely suspended thin films [35] and, with slight modifications, we can use the expression given there for the director angle correlation function. We have

$$G(\mathbf{q},\omega)\equiv\langle\theta(\mathbf{q},\omega)\theta(-\mathbf{q},-\omega)\rangle=\frac{2\Gamma k_B T}{\omega^2+\Gamma^2 K_b^2(q^2+\xi_+^{-2})^2}. \tag{B1}$$

Here $\theta(\mathbf{q},\omega)$ is the Fourier transform of $\theta(\mathbf{r},t)$ with two-dimensional wave vector $\mathbf{q}$ and frequency ω and Γ is a phenomenological kinetic coefficient (nonsingular at T_s) characterizing the relaxation of θ. Its inverse Γ^{-1} has the dimension (and physical meaning) of the torsional viscosity γ_1 in NLC's. Both coefficients (Γ and K_b) in Eq. (B1) are renormalized by disclinations.

The light-scattering cross section is obtained by evaluating the correlation function $\langle\epsilon_{\alpha\beta}(\mathbf{r},t)\epsilon_{\gamma\delta}(0,0)\rangle$. Consider, for example, an experimental configuration wherein the light is in the x-z plane and is initially polarized along y. Then the intensity $I(\mathbf{q},\omega)$ of scattered light due to orientational fluctuations is dominated by the correlation function

$$I(\mathbf{q},\omega)=M\langle\cos 2\theta(\mathbf{q},\omega)\cos 2\theta(-\mathbf{q},-\omega)\rangle, \tag{B2}$$

where $M=\epsilon_a^2\omega^4/8\pi^2c^4$ (ϵ_a is the dielectric anisotropy of the NLC, and c the velocity of light) is the standard prefactor relating light-scattering intensity to the fluctuation correlation function.

As shown in [24], $I(\mathbf{q},\omega)$ can be written in the form

$$I(\mathbf{q},\omega)=M\int d^2r\ dt\ \exp[-4g(\mathbf{r},t)+i\omega t-i\mathbf{q}\cdot\mathbf{r}], \tag{B3a}$$

with

$$g(\mathbf{r})=\frac{k_B T}{4\pi^2 K_b}\int\frac{d^2q}{q^2+\xi_+^{-2}}\times[1-\exp(-\Gamma K_b(q^2+\xi_+^{-2})t+i\mathbf{q}\cdot\mathbf{r})]. \tag{B3b}$$

Using Eqs. (B3), the wave vector dependence of the integrated intensity $I(\mathbf{q})=\int d\omega\ I(\mathbf{q},\omega)$ is

$$I(\mathbf{q})\propto\begin{cases} q^{-(2-x)} & \text{for } q\xi_+\gg 1\\ \xi_+^{-x}q^{-2} & \text{for } q\xi_+\ll 1,\end{cases} \tag{B4a}$$

with

$$x=2k_BT/\pi K_b. \tag{B4b}$$

It follows from Eq. (21) that, at $T=T_s$, $x=\frac{1}{4}$.

Similarly, the asymptotic dependence of $I(\mathbf{q},\omega)$ on $\mathbf{q}$ and ω can be derived in various limits [24]. The resulting expression are

$$I(\mathbf{q},\omega)\approx\begin{cases} M/\omega q^{2-x} & \text{for } q\xi_+\gg 1 \text{ and } \omega\gg\Gamma K_b\\ M/q^2(\Gamma K_b\xi_+^{-2})^{x/2}\omega^{1-(x/2)} & \text{for } q\xi_+\gg 1 \text{ and } \Gamma K_b\xi_+^{-2}\ll\omega\ll\Gamma K_b q^2\\ M/\omega q^2 & \text{for } q\xi_+\gg 1 \text{ and } \omega\ll\Gamma K_b\xi_+^{-2}\\ M/\omega\xi_+^x q^2 & \text{for } q\xi_+\ll 1 \text{ and all } \omega.\end{cases} \tag{B5}$$

Note that, in all these expressions for $I(\mathbf{q},\omega)$, the critical behavior near the BKT phase transition enters only via the temperature dependence of the correlation length ξ_+.

[1] P. Sheng, Phys. Rev. Lett. **37**, 1059 (1976).
[2] P. Sheng, Phys. Rev. A **26**, 1610 (1982).
[3] A. Mauger, G. Zribi, D. L. Mills, and J. Toner, Phys. Rev. Lett. **53**, 2485 (1984).
[4] R. M. Hornreich, Phys. Lett. **109A**, 232 (1985).
[5] M. Schick, Phys. Rev. Lett. **54**, 2169 (1985).
[6] H. Nakanishi and M. E. Fisher, Phys. Rev. Lett. **49**, 1565 (1982).
[7] J. Cahn, J. Chem. Phys. **66**, 3667 (1977).
[8] K. Miyano, Phys. Rev. Lett. **43**, 51 (1979).
[9] W. Chen, L. J. Martinez-Miranda, H. Hsiung, and Y. R. Shen, Phys. Rev. Lett. **62**, 1860 (1989).
[10] H. Hsiung, Th. Rasing, and R. Shen, Phys. Rev. Lett. **57**, 3065 (1986).
[11] P. G. de Gennes, Mol. Cryst. Liq. Cryst. **12**, 193 (1971).
[12] An additional symmetry-allowed elastic term $\frac{1}{2}\epsilon_{ij,k}\epsilon_{ik,j}$ is equivalent, after a double integration by parts, to a shift in the value of c_2 together with a (derivative dependent) surface term. The latter, however, does not contribute to the free energy when the order parameter is dependent upon only one spatial variable. We may therefore ignore this additional term.
[13] H. Grebel, R. M. Hornreich, and S. Shtrikman, Phys. Rev. A **28**, 1114 (1983).
[14] T. J. Sluckin and A. Poniewierski, in *Fluid Interfacial Phenomena*, edited by C. A. Croxton (Wiley, New York, 1985), p. 215.
[15] A. K. Sen and D. E. Sullivan, Phys. Rev. A **35**, 1391 (1987).
[16] T. Moses and Y. R. Shen, Phys. Rev. Lett **67**, 2033 (1991).
[17] G. P. Crawford, R. Ondris-Crawford, S. Zumer, and J. W. Doane, Phys. Rev. Lett **70**, 1838 (1993); Phys. Rev. E **53**, 3647 (1996).
[18] T. J. Sluckin and A. Poniewierski, Phys. Rev. Lett. **55**, 2907 (1985).
[19] V. L. Berezinskii, Zh. Éksp. Teor. Fiz. **61**, 1144 (1971) [Sov. Phys. JETP **34**, 610 (1971)].
[20] J. M. Kosterlitz and D. J. Thouless, J. Phys. C **6**, 1181 (1973).
[21] J. M. Kosterlitz, J. Phys. C **7**, 1046 (1974).
[22] Y. L'vov, R. M. Hornreich, and D. W. Allender, Phys. Rev. E **48**, 1115 (1992). Note that the definitions of the surface interaction coupling parameters in this and the following two references are slightly different from those used in the present paper.
[23] N. Kothekar, D. W. Allender, and R. M. Hornreich, Phys. Rev. E **49**, 2150 (1994).
[24] R. M. Hornreich, E. I. Kats, and V. V. Lebedev, Phys. Rev. A **46**, 4935 (1992).
[25] U. Ascher, J. Christiansen, and R. D. Russel, ACM Trans. Math. Software **7**, 209 (1981)
[26] U. Ascher, R. M. M. Mattheij, and R. D. Russel, *Numerical Solution of Boundary Value Problems for Ordinary Differential Equations* (Prentice Hall, Englewood Cliffs, NJ, 1988), pp. 486–490.
[27] This result is obtained by regarding the system as symmetric about $\zeta=0$, with the surface interaction existing in an infinitesimal region centered about this point (see, e.g., Refs. [4,22,24]). Alternate definitions are possible; they effect the connection between the phenomenological coupling parameters ν, ν_1, and ν_2, and the physical interaction potential at the surface.
[28] D. L. Stein, Phys. Rev. B **18**, 2397 (1978).
[29] P. Sheng, B. Z. Li, M. Zhou, T. Moses, and Y. R. Shen, Phys. Rev. A **46**, 946 (1992).
[30] H. J. Coles, Mol. Cryst. Liq. Cryst. **49**, 67 (1978).
[31] E. Dubois-Violet and O. Parodi, J. Phys. (Paris) Colloq. **30**, C4-57 (1969).
[32] V. M. Pergamenschchik, Phys. Rev. E **48**, 1254 (1993).
[33] H. Yokoyama, J. Chem. Soc. Faraday Trans. 2 **84**, 1023 (1988).
[34] H. Yokoyama, Mol. Cryst. Liq. Cryst. **165**, 265 (1988).
[35] S. W. Heinekamp and R. A. Pelcovits, Phys. Rev. B **32**, 2506 (1985).